



Relationships between Snowfall Densities and the Main Types of Solid Hydrometeors Deduced from Measured Size and Fall Speed, for snowpack modeling applications

5 Masaaki Ishizaka¹, Hiroki Motoyoshi¹, Satoru Yamaguchi¹, Sento Nakai¹, Toru Shina², Ken-ichiro Muramoto³

¹Snow and Ice Research Center, National Research Institute for Earth Science and Disaster Resilience, Nagaoka, 940-0821, Japan

²Department of Electronics and Computer Engineering, Toyama National College of Technology, Toyama, 933-0293, Japan

10 ³Kanazawa University, Kakuma-machi, Kanazawa, 920-1192, Japan

Correspondence to: Satoru Yamaguchi (yamasan@bosai.go.jp)

Abstract. Initial densities of deposited snows mainly depend on hydrometeors types of snowfalls. Some previous researchers qualitatively indicated their relations. However a quantitative relationship between snowfall densities and hydrometeors types had not been established because of difficulty in parameterizing varieties of types of hydrometeors in a snowfall event. Thus in a previous study, we introduced a new variable, CMF (Center of Mass Flux distribution), which described the hydrometeors mainly contributing to a snowfall. The CMF is a set of the averages of the size and the fall speed weighted by the mass flux estimated from all measured hydrometeors in a snowfall. It represents the predominant type of hydrometeors of the snowfall quantitatively. In this study, we examined the relationships between the densities of newly fallen snows and their predominant snow types as indicated by the CMFs. We measured the snowfall densities, simultaneously observing the size and the fall speed of the hydrometeors of the snowfalls and deduced the predominant hydrometeor types of each snowfall event from their CMFs. The measurements of snow densities were carried out for short periods, 1 or 2 h, during which the densification of the deposited snows was negligible. We also selected cases when snowfalls contained basically the same type of hydrometeors. As a result, we could obtain the relationships between the main snow types and the snowfall densities not only qualitatively reported by previous researchers but also the quantitative relationships between snowfall densities and the CMF-densities, which were a presumed density derived from the size and mass components of the CMFs. This suggests the possibility of estimating snowfall densities, which reflected snow types (the main types of hydrometeors), directly from the measured size and the fall speed data, and using them as the initial densities for a snow pack in a numerical model, even though difficult issues remain in parameterization for a practical use. Our results might be applicable only to temperate snow at our observation site, Nagaoka, 37°N, where riming and aggregation are predominant. However the methodology in this study would be useful for other kinds of snow.



1 Introduction

The density of newly fallen snow is an important physical property of deposited snow as it begins to change as soon as the snow falls on the ground. The snowfall density is thought to be determined first by the types of hydrometeors and their dimensions. Some researchers have attempted to study the relationships between the densities of newly fallen snow and their snow crystals or the types of snow in falling snows.

Power et al. (1964) examined snowfall density related to the snow crystal forms and their riming properties within general storm conditions in Canada. They reported relationships between the predominating snow crystals and the snowfall density in each snow storm. The values of snow densities varied and were distributed over wide ranges according to the predominant snow type. Their data showed that the density of snow consisting of dendritic snow crystals was lower than that of snow consisting of plate and column type crystals and that riming affected an increase in density.

Kajikawa et al. (1989) investigated the relationships between snow density and the predominant snow crystal types considering the degree of riming, the air temperature, and the wind packing. Their results were similar to those of Power et al. (1964) relating to snow crystal type.

Kajikawa et al. (2006) further examined snow crystal types as well as other factors affecting snow density. These factors were the horizontal size distribution, the contribution rate of graupel, and the kinetic energy flux to the snow surface brought by falling particles. They obtained some important results, including the strong dependence on kinetic energy. However, their observation intervals of about 6 h were so long that snowfalls could not be consisted of a single kind of snow crystal represented as the main type. Snow types were thought to change during long observation periods, and a complicating snowpack had formed. Therefore, they did not have consistent results, even though certain aspects of their investigations were very important.

To clarify the relationships between snowfall densities and snowfall properties, we need to measure densities of similar types of hydrometeors, as well as their dimensions.

As is generally known, snowfalls consist of hydrometeors of various sizes, with small sizes being abundant. Therefore, Ishizaka et al. (2013) presented a new variable to quantitatively describe the main types of hydrometeors in snowfall considering the contribution of all hydrometeors to the precipitation. In their method, a main snow type of a snowfall is indicated with a pair of two elements, size and fall speed, which are obtained by averaging the size and the fall speed weighted with their mass flux for all measured hydrometeors. The pair is called a Center of Mass Flux (CMF) distribution. Since size-fall speed relationships of hydrometeors represent their particle types well, we can deduce a main snow type in a snowfall from the location of the CMF in the size-fall speed coordinates.

In this work, we characterize main snow types of snowfalls with the CMFs instead of snow crystal types and present their quantitative relationships with their snowfall densities. If quantitative relationships between densities and CMFs of snowfalls exist, we would be able to estimate the densities of deposited snows directly from the measured size and fall speed using the quantitative relationships..



Recently, a variety of disdrometers, which can automatically measure the sizes and the fall speeds, like Parsivel (OTT Hydromet GmbH; Löffler-Mang and Joss, 2000) and two dimensional disdrometers (Kruger and Krajewski, 2002), have been developed; and the measurement of the size and fall speed of snows have been made. Therefore, we can continuously estimate the densities of accumulated snows using these apparatuses and the relationships established here, and use them as the initial densities of newly fallen snows in a numerical snowpack model. In this article we will briefly mention about application of the relationships to a snowpack model along with difficulty in parameterization for a practical use

2 Observations of densities and measuring system for falling snow properties

Observations of the main types of snow falls and the density of newly fallen snows were carried out at the Falling Snow Observatory (FSO) of the Snow and Ice Research Center at the National Research Institute for Earth Science and Disaster Prevention (NIED) in Nagaoka, 37°N, Japan, which belongs to the temperate climate zone, in the winter seasons from 2013 to 2015. The FSO is located in a coastal area facing the Sea of Japan, where the Siberian monsoon brings heavy snowfalls in winter. The winter temperature, around 0 °C, allows aggregation to be generally predominant as well as riming.

2.1 Measurements of Snowfall density

The measurement of the densities of the newly fallen snows was carried out at our low-temperature room where the temperature was kept at about -5°C. The low-temperature room has an opening (1.2 m × 0.6 m) on the roof, through which snows falling and accumulate on a flat table in the room. We obtained the density of the accumulated snows by measuring the snow depth and the snow weight sampled with a cylindrical sampler of 10 cm diameter (Fig. 1). We sampled accumulated snows three or four times by selecting undisturbed areas of the snow cover on the table. The snow depth was measured at four points around the sampler at each sample point with a ruler with a minimum scale of 1 mm. These four measurements were then averaged. The density of snow was calculated from the following formula:

$$\rho = \frac{W}{S \cdot h}, \quad (1)$$

where W is the weight of the snow, S is the cross section of the sampler, and h is the height of the accumulated snow.

2.2 Observations of snowfalls and determination of the main type of hydrometeors of each snowfall event

Since the methods of both observation and determination of the main type of hydrometeors are almost same as reported in the previous study that introduced the CMF (Ishizaka et al., 2013), we briefly describe the observation procedure here.

The measurements of snowfalls were carried out at the FSO with an automated system (Muramoto et al., 1989, 1993) placed in a space enclosed by double-net fences and detects falling snow particles falling under regulated wind conditions with a CCD camera and image processing. The size and the fall speed of every detected hydrometeors were obtained from the recorded data. We use the maximum horizontal width of the particle as the size of a particle with a resolution of 0.25 mm. The fall speeds were also calculated from the vertical displacement of a particle in consecutive frames captured by the CCD



camera with an interval of 1/60 seconds. The resulting resolution of fall speed is 0.03 m/s. This system is regarded as a disdrometer with a bin of 0.25 mm in size and 0.03 m/s in fall speed.

Using this system, we could obtain the distributions of the size and the fall speed of hydrometeors in a targeted snowfall corresponding to each bin at 1 min interval. The predominant snow types were determined by calculating the CMFs from the data, since the locations of CMFs in the size-fall speed coordinates characterize a predominant snow type well (Ishizaka et al., 2013). In this work, the main types of hydrometeors are represented by indicating the locations of CMFs instead of describing the predominant snow crystals like previous researchers (Power et al., 1964; Kajikawa et al., 1989). For example, in Fig. 2, the CMFs of two snowfall events, A13 and G4, listed in Table 1, are shown along with all measured sizes and fall speeds of the falling snows. It is found that the location of the CMFs differ from each other according to their difference in the types of hydrometeors, i.e. aggregate type (A13) and graupel type (G4).

2.3 Selection of snowfall events

With regards to meteorological conditions, we selected events when the air temperature was below 0°C during the entire period of the observations to avoid cases in which melting of the snow occurs. Wind conditions were not taken into consideration because the measurements of the densities were carried out under the calm air condition in the cold-room. Even if the observation periods were short, 1 or 2 h for almost all events, snow types varied. To examine the variations, the CMFs integrated over the whole period and the CMF of every 1 min interval (1min-CMF) in the snowfall were considered. The 1 min-CMFs generally varied in all cases according to slight changes either in the size or the fall speed. Therefore, by assessing both the integrated CMF and the 1 min-CMFs, we selected cases in which snowfalls were regarded to be consistent in snow types, even if changes in size were recognized. If different snow types having the almost same contribution to precipitation were mixed, the 1min-CMFs would vary at different areas in the size-fall speed coordinates, while the integrated CMF of the event is located at an intermediate area. Such cases must be eliminated from the targeted events. Figure 3 shows one of the eliminated events, as well as a selected one. In Figure 3 a, the 1-min CMFs scatter into two areas corresponding to graupel and aggregate, and the integrated CMF locates at an intermediate region. In this situation, we can recognize that two different types of snows were falling with almost the same intensity during the event. This event was eliminated. In Figure 3b, both the 1 min-CMFs and integrated CMF shows that aggregates, with the degree of riming not so heavy as a densely rimed one, fell but changed their size. This case was selected because the snow type was almost the same even though the size of the particles had changed.

2.4 Estimation of errors in density measurements

Although we sampled snow three or four times for each snow event as mentioned above in section 2.1 and averaged them, some errors were expected when we read the scale on the ruler. From Eq. (1), we could estimate this error as it relates to density, $\Delta\rho$, using the following equation,



$$\Delta\rho = -\frac{W}{s \cdot h^2} \cdot \Delta h, \quad (2)$$

The reading error in density was estimated by Eq. (2), setting Δh to +/- 1 mm. Eq. (2) indicates that smaller depths give larger errors, and this relates to errors in density. Therefore, it is preferable to wait until snows accumulate adequately. However, if we take a long time in this process, a variety of snow types is likely to mix in one snowfall case. Therefore, we restricted the observation period to about 2 h or less with the exception of two graupel cases (Table 1). Thus, when the snow depths of some events were less than 10 mm and the errors calculated were more than 10% of their density, we reflected this in the error bars of the graphs in a later section.

Concerning the accuracy in density measurements, there is another rather complicated situation that we must also consider. It is caused by the densification of accumulated snow. We will estimate it as follows.

10 Assuming visco-elastic theory, a distortion in the height of snow linearly increases with stress, σ .

$$-\frac{1}{h} \left(\frac{dh}{dt} \right) = \frac{1}{\eta} \sigma, \quad (3)$$

where η is the coefficient of the viscosity of snow.

Adapting Eq. (3) for an accumulated snow of density ρ , we obtain the following equation;

$$\frac{1}{\rho} \left(\frac{d\rho}{dt} \right) = W_{press} \cdot g, \quad (4)$$

15 where W_{press} is weight of the compressing snow in the unit area and g is the constant of gravity. In Endo et al. (1990), for densities of 50–180 kg/m³, η is expressed as,

$$\rho = C\rho^4, \quad (5)$$

where the coefficient, C , varies with snow temperature, crystal types, etc. and has a value of 0.392 on average. Substituting η from Eq. (5) in Eq. (4), we can obtain the following solution,

$$20 \rho_t = \left(4 \int_{t_0}^t \frac{1}{C} W_{press} \cdot g dt + \rho_{t_0}^4 \right)^{\frac{1}{4}} \quad (6)$$

Estimating the difference between ρ_t and ρ_0 with Eq. (6), we find that the differences are not large compared with the reading errors discussed previously during such short period observations. For example, assuming it snows at a constant rate of 3 mm per hour (heavy snowfall) and the resultant density ρ_t reaches 60 kg/m³ (a general value), we can obtain the calculated ρ_0 with Eq. (6), as 59.4 kg/m³ and 58.7 kg/m³ at accumulation intervals of 1 h and 2 h, respectively. The differences are a

25 small percentage of the obtained density and one order of magnitude smaller than that originated from the reading error mentioned above. Therefore, we consider the densification errors to be negligible.



3 Results and discussion

3.1 Classification of snowfall events

In previous research (Power et al. 1964; Kajikawa et al., 1989), identification of the main snow types was based on the snow crystal types in the snowfalls. However, our identification is not based on crystal types, but on the locations of the CMFs in the size-fall speed coordinates, which change and differ with respect to the main hydrometeor types. Therefore, we classified the types into four groups: aggregate, graupel, and two small groups, based on locations of the CMFs in the size-fall speed coordinates as illustrated in Figure 4.

The graupel and both the aggregate group and the two small groups are divided by the boundary that expresses the size-fall speed relationship for graupel-like snow of the lump type reported by Locatelli and Hobbs (1974) (we sometimes refer to it as L&H, 1974 in Figures). Further, the aggregate group and the two small groups are divided by their size. If a size component of the CMF is larger than 4 mm, it is classified into the aggregate group. In our previous study (Ishizaka et al., 2013), the CMFs of the aggregate type of snowfall have been larger than 4 or 5 mm in their size component. Hence, we adopted this criterion, though it is rather subjective. In addition, the small group is divided into two groups, small group 1 and 2, with the boundary corresponding to the size-fall speed relationship for graupel-like snow of hexagonal type (Locatelli and Hobbs, 1974).

The densities of the snowfall events classified by the above procedure are listed in Table 1. Table 1 also shows the CMF, the measured snow depth, the sampling weight, and the CMF-densities (explained in section 3.4).

3.2 Snowfall densities of the aggregate group and the small group 1

Figure 5 shows the distributions of the densities of all groups with error bars originating from the reading errors. The minimum of the densities in the aggregate group including small group 1 (referred to as S1 group) is 17.9 kg/m^3 for A3, and the maximum density is 94.6 kg/m^3 for A14. The densities mainly range between ~ 30 – $\sim 70 \text{ kg/m}^3$. This tendency coincides with the frequency of density ranges reported by Power et al. (1964) and Kajikawa et al. (1989), although rather larger densities of riming particles were listed in the former. A minimum value of 25 kg/m^3 is reported in the latter study for the case of an unrimed stellar crystal and 30 kg/m^3 in the former study for an unrimed dendrite. These minimums are close to our minimum, 17.9 kg/m^3 , which is the smallest of all measured densities in our observations. Moreover, these smaller values of about 20 kg/m^3 are also near to the density of a single hydrometeor of unrimed or slightly rimed aggregate obtained by 3-D microphotograph analysis, as reported by Ishizaka (1995).

In Figure 6, the locations (the size and the fall speed) of CMFs for A and S1 groups are plotted with their densities expressed by grey-scale shading. The figure shows that the fall speed of the highest density event, A14, is the largest of all events and that the CMF is located near the empirical relation curve of the densely rimed aggregate (Ishizaka, 1995). In contrast, the fall speed of the lowest density event, A3, is lower than that of the moderately rimed aggregate (Ishizaka, 1995). It indicates



particles in the event (A3) has a low riming property. And the size of the CMF for A3 is the largest of all. The CMFs of the others locate at a lower range in the fall speed than that of A14 and at a smaller range in size than that of A3. From these results, we find that density depends on both the degree of riming and the size. The strong effect of riming on the increase in snowfall density was emphasized in previous research (Power et al., 1964; Kajikawa et al., 1989). The relation that density decreases as the dimension of an aggregate increases was also reported by Ishizaka (1993) for a single aggregate.

3.3 Density of the graupel group and the small group 2

In our classification based on CMFs, the snowfalls that consisted mainly of graupel can be easily selected by the simple criteria previously mentioned. The densities of their events are listed in the graupel group in Table 1 and Figure 5, as well as in small group 2 (referred to as the S2 group). The densities of the graupel group range from about 40 to 150 kg/m³ and are generally higher than that of the aggregate group. This tendency is understandable because of the strong dependence of density on the riming property as described in the previous section. The highest densities are given as 143 kg/m³ in the graupel group and are near to the result reported by Kajikawa et al. (1989) of 120 kg/m³.

We also find the error bars for events in the graupel group are generally larger than that for aggregate group. The reason is that the height of the snow is relatively lower by weight for graupel than for aggregate. Therefore, the errors which are in proportion to weight and inversely proportional to height, as indicated in Eq. (2), are generally large in the graupel cases.

In Figure 7, the locations (the size and the fall speed) of CMFs for G and S2 groups are plotted with their densities expressed by grey-scale shading. In the figure, the three curves which represent the size-fall speed relationships for different types of graupels (Locatelli and Hobbs, 1974) are illustrated. The fall speed of the lump type graupel is the highest and that of the hexagonal type is the lowest. The conical graupel has an intermediate fall speed by size. These differences are thought to be caused by their shapes and mainly by their particle densities. A larger density particle has a higher fall speed at the same size. It is found that the densities of G and S2 groups have the same tendency that the higher density is, the larger the fall speed the curve in the vicinity of the CMF for an event has. This tendency is understandable, because the accumulated snow consisting of heavier graupels has a larger density.

3.4 Relationships between snowfall density and CMF-related quantity (CMF-density)

In the previous sections, we find that CMFs are one of the quantitative factor which can reasonably explain snowfall density. However, it is preferable to establish quantitative relationships between snowfall densities and the CMF-related quantities. Therefore, we introduce “CMF-density” in the next section.

3.4.1 CMF-density

The CMF is calculated from the measured size and the fall speed of hydrometeors to average them by weighting their mass flux, which is defined as a product of mass and fall speed. In this process, the mass flux table, which indexes the calculated mass flux for each bin of a given size and a fall speed, is used to determine the mass flux of each hydrometeor (Ishizaka et



al., 2013). Figure 8a shows a graphical expression of the table, referred to as a “mass flux chart”. From the mass flux table, we can calculate mass for each bin, dividing the mass flux by the fall speed, resulting in a “mass table”. Thereby, we can obtain the mass for a given size and fall speed of a CMF. With the obtained mass, we introduce a new variable, “CMF-density”.

- 5 The CMF density, ρ_{CMF} , is defined as the presumed density calculated by dividing mass, m , by the volume of the sphere with a diameter of size, d , as in the following equation.

$$\rho_{CMF} = \frac{m}{\left(\frac{4}{3}\pi\left(\frac{d}{2}\right)^3\right)} \quad (7)$$

Using Eq. (7), we can obtain ρ_{CMF} for each bin, which results in a density table. Figure 8b shows a graphical expression of the density table, i.e. the “density chart”. Referring to the density table, we can obtain the CMF-density that corresponds to the integrated CMF of a snowfall event and examine the relationship with the measured snowfall density. As inferred from the definition of ρ_{CMF} , the CMF-density can be thought of as a presumed density of the main hydrometeor type which has a given size and fall speed corresponding to the location of the size-fall speed coordinates.

3.4.2 Relationships between snowfall density and CMF-density

Figure 9 shows the relationships of measured density (real density) vs. CMF-density for the aggregate group and for the graupel group. The plots of the two different groups are separated at the boundary of CMF-density, about 40 kg/m^3 . For both groups, real density increases with CMF-density. As a first approximation, we can obtain a curve for each group to fit the data using the Levenberg-Marquardt method. A power law function was adopted, since the curves were thought to start at the origin. The curves fairly represent the relationships between real density and CMF-density, although the values scatter around the curves to some extent.

20 One reason why the relationships differ from each other may be related to a different packing mechanism during the accumulation of different types of hydrometeors (Fig. 10). In the aggregate case, hydrometeors themselves have vacant spaces that affect the density of accumulated snow. On the other hand, graupels do not have such vacant space, even if the graupels themselves are somewhat porous. In a graupel case, the densities of the graupels themselves and the void space between them affect the snowfall density. And the former is thought to strongly affect the density of a graupel event.

25 In Figure 11, the densities of the snowfall events belonging to the S1 and S2 group are plotted along with the fitted curves for the aggregate group and the graupel group. In these cases, the densities of the two groups are separated significantly. This indicates that the classification process mentioned in section 3.1 is reasonable and that the S1 group has an affinity with the aggregate group and the S2 group has an affinity with the graupel group. However, the relationships between real densities and CMF densities are not clear when comparing the aggregate and graupel cases. The real density of the S1 and S2 groups is lower than that of the aggregate and graupel groups at the same CMF-densities, respectively. For the S1 group, the real densities are about 14% to 50% lower than that of the fitted curve of the aggregate group, and for S2 group, the real densities are also about 15% to 30% lower than that of the graupel group.



In these small particle groups, the snowfalls are mainly formed with small particles which have a variety of characteristics that cannot be clearly discerned, so that it might be difficult to establish clear relationships. Moreover, this uncertainty has originated, not only from the variety of snow types, but from the uncertainty in the mass flux chart (Ishizaka et al., 2013). This is because, in the small particles regions, relevant relationships between the mass, the size, and the fall speed have not
5 been established. Further research is needed in these targets.

3.5 A prospect for improvement of an initial density for use in a numerical snow pack model

In current numerical snow pack models, an initial density of a snowpack is generally derived from meteorological conditions such as the air temperature, the wind speed, etc. (Lehning et al., 2002; Vionnet et al., 2002; Yamaguchi et al., 2004). However, in the process, no snow types for newly fallen snows are considered, even though snowfall densities vary widely
10 according to the main snow types as seen in our results. Thus it is preferable to introduce a factor that reflects the snow types into estimation of the initial density of a snowpack model.

Our results show the possibility of estimating snowfall density, which reflects the main type of snows, by measuring the size and the fall speed of the hydrometeors in the snowfall. Therefore we could introduce the snowfall density, as such a factor, which reflects the snow types practically by assessing the real time data derived from a disdrometer, which has been
15 developed recently, throughout the quantitative relationships between the snowfall densities and the CMF-densities. This process should improve the accuracy of the initial density of a snowpack in a numerical model. Since snow types change greatly in a short period, it would be better to estimate the densities from the CMF-densities for a short time interval, for example less than 5 min, even though some uncertainty remains in the small size particle groups. For these small particles, temporal relationships might be needed.

20 In addition, the CMF reflects information about the shapes of particles so that it may be possible to reflect it to shape factors like sphericity or dendricity in a snow pack model. Moreover information about hydrometeor itself is also important for avalanche warning, because some avalanches are induced by falling snows which include particular types of hydrometeors, such as a large graupel, a nonrimed stellar crystal, and a very low density snow.

In any case how to parameterize these factors in a snowpack model is important issue, but some difficulties exist. The factors
25 originated with hydrometeors types mentioned here, such as snowfall density, are relating to an initial state of a deposited snow, while the variables used for estimating the density in a general snowpack model (Lehning et al., 2002), such as air temperature or surface temperature, are relating to not only initial state but also consecutive state during a discretization interval of the model. On the other hand hydrometeors types would certainly affect a metamorphosing process. Initial snowpack mainly consisted of a graupel type snow would differently develop from that consisted of an aggregate type snow.

30 In this way the factors for hydrometeors types also have an indirect influence on the consecutive state, but it has not been clear how affect the hydrometeors types on the metamorphosing process. Further studies are needed on the issue.

In this study a wind effect on the density was not taken into consideration, though the initial density is strongly affected by wind speed throughout packing and transportation of snow (Vionnet et al., 2013). Wind has a direct influence on the density



of an initial state and important factor, but the effect should be treated with respect to the hydrometeors types. Therefore we have firstly established the quantitative relationships between the densities and hydrometeors types without wind. To clarify the wind effect with respect to the hydrometeors types is one of targets in our next studies.

4 Summary

5 In this study, we tried to establish quantitative relationships between snowfall densities and the main types of hydrometeors in snowfalls. The main hydrometeor types were indicated with the integrated CMFs for the snowfall events instead of describing the predominant snow crystals as reported in previous studies (Power et al., 1964; Kajikawa et al., 1989).

In our observations, snowfall events that consisted of almost the same type of snow were selected by assessing both the CMFs at a short time interval and an integrated one. Sampling periods for density observations were set within about 2 h, except for a few events to avoid the densification of the accumulated snows. These short time intervals were also favourable in the selection of the similar type snow events.

The observations brought the following results:

1. Snowfall densities ranged from about 20 to 100 kg/m³ in the case of the aggregate type of snow, and from about 40 to 150 kg/m³ in the case of the graupel type of snow. These values almost coincided with those reported by previous researchers (Power et al., 1964; Kajikawa et al., 1989).

2. The densities of the aggregate group were affected by both the degree of riming and size. As the denser snows are rimed, the densities of the accumulated snows are higher. The densities decrease as the size of the hydrometeors in the snows increase.

3. The densities of snowfalls belonging to the graupel group depended mainly on the weights (densities) or hardness of the graupel themselves which changed according to their types ranging from the hexagonal type (soft) to the lump type (hard).

4. To establish quantitative relationships between observed snowfall densities and snow types (hydrometeors), a CMF related quantity, CMF-density, was introduced.

5. Quantitative relationships between the observed densities and the CMF-densities were obtained. The relationships differed by hydrometeors types, giving a different relationship for the aggregate group as compared to the graupel group. The difference could be thought to originate from a difference in their packing processes.

These results showed that the CMF method that indicates both the main types of snow as well as the representative size quantitatively is a reasonable means of establishing quantitative relationships between the snowfall density and the characteristics of snowfall. From the quantitative relationships, we showed the feasibility of using the relationships to give an initial density for a numerical snow pack model by assessing the size and the fall speed data from a disdrometer.

Moreover, we also showed the possibility that the CMF method could improve shape factors like sphericity or dendricity for the initial state of snows in the snow pack model, even though for practical use further studies are needed to parameterize these factors with integrating other meteorological factors. Uncertainty in the relationships for the small particles region is



also another problem as well as melting snow because, in colder regions, like alpine site, the sizes of falling snows might be smaller. Further studies are needed to solve these issues.

Acknowledgments

The authors thank Florent Domine, Co-Editor in chief, for his constructive review and helpful advice. This research is supported by a project of the National Research Institute for Earth Science and Disaster Prevention (NIED) "Research on advanced snow information and its application to disaster mitigation", and JSPS, KAKENHI grant Numbers 26560195, 15H01733.

References

- Endo, Y., Ozeki, Y., and Niwano, S.: Relation between compressive viscosity and density of low-density snow. *Seppyo*, 52, 267-274 (in Japanese), doi:10.5331/seppyo.52.267, 1990.
- Ishizaka, M.: Accurate measurement of snowflake densities using 3-D microphotographs. *Ann. Glaciol.*, 18, 92-96, 1993.
- Ishizaka, M.: Measurement of falling velocity of rimed snowflakes. *Seppyo*, 57, 229-238 (in Japanese), doi:10.5331/seppyo.57.229, 1995.
- Ishizaka, M., Motoyoshi H., Nakai S., Shiina T., Kumakura T., and Muramoto K.: A New Method for Identifying the Main Type of Solid Hydrometeors Contributing to Snowfall from Measured Size-Fall Speed Relationship. *J. Meteor. Soc. Japan*, 91, 747-762, doi:10.2151/jmsj.2013-602, 2013.
- Kajikawa, M.: Relationship between new snow density and shape of snow crystals. *Seppyo*, 51, 173-183 (in Japanese), doi:10.5331/seppyo.51.178, 1989.
- Kajikawa, M., Goto H., Saruwatari T., Kanaya K., Hashimoto M., and Kikuchi K.: Studies on the characteristics of snow particles affecting new density. *Seppyo*, 67, 213-219 (in Japanese), doi:10.5331/seppyo.67.213, 2005.
- Kruger, A. and Krajewski W. F.: Two dimensional video disdrometer: A description. *J. Atmos. Oceanic Technol.*, 19, 602-617, doi:10.1175/1520-0426(2002)019<0602:TDVDAD>2.0.CO;2, 2002.
- Lehning M., Bartelt P., Brown B., and Fierz C.: A physical SNOWPACK model for the Swiss avalanche warning Part III: meteorological forcing, thin layer formation and evaluation. *Cold Reg. Scie. Technol.*, 35, 169-184, doi:10.1016/S0165-232X(02)00072-1, 2002.
- Locatelli J. D., and Hobbs P. V.: Fall speed and mass of solid precipitation particles. *J. geophys. Res.*, 79, 21885-2197, doi:10.1029/JC079i015p02185, 1974.
- Löffler-Mang M., and Joss J.: An optical disdrometer for measuring size and velocity of hydrometeors. *J. Atmos. Oceanic Technol.*, 17, 130-139, doi:10.1175/1520-0426(2000)017<0130:AODFMS>2.0.CO;2, 2000.



Power B. A., Summers P. W., and D'Avignon J.: Snow crystal forms and riming effect as related to snowfall density and general storm conditions. *J. Atmos. Scie.*, 21, 300-305, doi:10.1175/1520-0469(1964)021<0300:SCFARE>2.0.CO;2, 1964.

Muramoto, K., Shiina T., Endo T., Konishi H., and Kitano K.: Measurement of snowflake size and falling velocity by image processing. *Proc. NIPR Symp. Polar Meteorol. Glaciol.*, 2, 48-54, 1989.

5 Muramoto, K. and Matsuura K.; A computer database for falling snowflakes. *Ann. Glaciol.*, 18, 11-16, 1993.

Vionnet, V., Brun F., Morin S., Boone A., Faroux S., Le Moigne P., Martin E., and Willemet J. M. : The detailed snowpack scheme Crocus and its implementation in SURFEX v7.2. *Geosci. Model Dev.*, 5, 773-791, 2012, doi:10.5194/gmd-5-773-2012.

10 Vionnet, V., Guyomarc'h G., Naaim Bouvet F., Martin E., Durand Y., Bellot H., Bel C., Pugliese P. : Occurrence of blowing snow events at an alpine site over a 10-year period: Observations and modelling. *Adv. Water Resour.*, 55, 53-63, 2013, doi: 10.1016/j.advwatres.2012.05.004.

Yamaguchi, S., Sato A., and Lehning M.: Application of the numerical snowpack model (SNOWPACK) to the wet-snow region in Japan. *Ann. Glaciol.*, 38, 266-272, doi:10.3189/172756404781815239, 2004.

15

20

25

30



Table 1: Snowfall events classified into four groups, their observation periods, the snowfall densities, the CMFs, the depths of the accumulated snow, the sampling weights, and the CMF-densities.

event	period (Japan Standard Time)	density (kg/m ³)	CMF		sampling snow depth (mm)	sampling weight (g)	CMF- density (kg/m ³)
			size (mm)	fall speed (m/s)			
Aggregate group							
A1	10 Jan. 2013 10:30–11:30	43.8	5.5	1.0	29.5	10.2	19.9
A2	10 Jan. 2013 16:22–17:15	34.7	6.6	1.0	37.4	10.2	15.4
A3	17 Jan. 2013 16:18–17:10	17.9	7.6	0.9	18.3	2.6	12.2
A4	06 Feb. 2013 08:31–11:05	70.6	4.2	1.1	27.5	15.5	28
A5	20 Feb. 2013 13:35–14:10	62.9	5.8	1.1	21.1	10.4	18.7
A6	09 Jan. 2014 14:41–15:54	40.7	4.8	1.0	9.3	3.0	22.1
A7	10 Jan. 2014 09:45–11:15	62.6	4.2	1.1	17.8	8.8	27.8
A8	10 Jan. 2014 16:10–17:10	52.9	4.5	1.1	22.8	9.3	25.9
A9	17 Jan. 2014 14:05–15:02	42.8	6.0	1.1	19.8	6.7	17.3
A10	06 Mar. 2014 16:20–17:10	62.5	4.0	1.2	13.5	6.4	30.3
A11	07 Mar. 2014 09:00–09:55	51.8	4.1	1.2	11.0	4.5	30.3
A12	07 Mar. 2014 17:20–18:05	55.2	4.6	1.0	20.0	8.7	23.2
A13	11 Mar. 2014 10:07–10:50	49.2	6.0	1.0	23.0	9.1	18.0
A14	22 Dec. 2014 11:25–12:05	94.6	4.4	1.4	17.0	12.1	37.0
Graupel group							
G1	18 Jan. 2013 11:11–14:00	77.6	4.0	1.8	3.9	2.3	51.6
G2	18 Jan. 2013 14:03–16:35	95.1	3.6	2.0	4.6	3.3	64.3
G3	20 Feb. 2013 13:08–13:28	135.1	2.9	2.0	19.1	20.2	77.3
G4	10 Jan. 2014 13:15–14:06	143.1	3.6	2.6	25.8	28.7	89.5
G5	10 Jan. 2014 15:13–16:05	139.7	2.2	1.7	17.3	18.6	91.6
G6	10 Mar. 2014 12:40–13:40	48.7	4.1	1.5	5.5	1.8	44.2
G7	17 Dec. 2014 15:33–16:26	100.8	2.3	1.5	19.3	14.9	70.6
G8	17 Dec. 2014 16:31–17:23	99.4	2.6	1.7	14.8	11.6	69.0
G9	10 Feb. 2015 09:05–10:05	92.6	3.9	2.2	13.3	9.6	69.4
Small group1							
S1-1	06 Feb. 2013 12:32–13:32	68.6	3.0	1.1	25.7	13.9	38.1
S1-2	17 Jan. 2014 13:11–14:00	73.7	3.1	1.1	24.0	14	40.0
S1-3	05 Feb. 2014 09:22–10:30	42.8	3.9	1.0	16.7	5.5	28.9
S1-4	05 Feb. 2014 10:40–11:40	33.2	3.8	1.0	9.3	2.4	28.9
S1-5	05 Feb. 2014 11:50–13:15	32.9	3.8	1.0	10.3	2.6	29.2
S1-6	09 Feb. 2015 16:33–17:00	57.2	3.8	1.1	16.5	7.4	29.6
S1-7	09 Feb. 2015 17:19–17:40	55.4	3.4	1.1	19.3	8.1	35.2
Small group2							
S2-1	09 Jan. 2014 15:58–16:55	57.8	2.9	1.3	6.3	2.4	59.0
S2-2	04 Feb. 2014 14:12–15:15	69.0	2.3	1.1	13.5	7.1	59.5
S2-3	08 Mar. 2014 09:50–11:00	74.4	2.3	1.2	5.0	2.9	72.4
S2-4	28 Jan. 2015 08:42–09:40	86.5	2.4	1.3	14.3	8.9	71.2



5 **Figure 1: Accumulated snow on the thin metal plate on the table in the low-temperature room and the cylindrical sampler.**

10

15

20

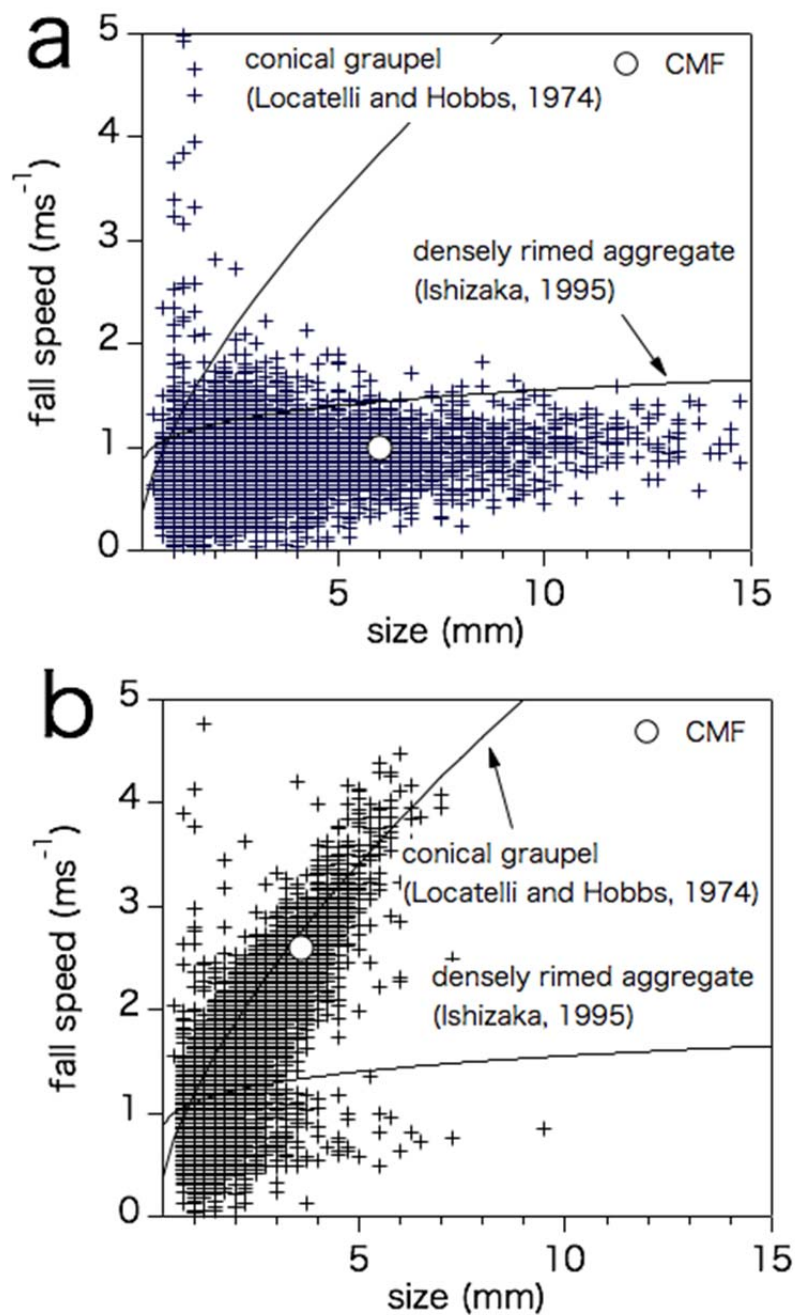


Figure 2: The distributions of measured sizes and fall speeds, and the integrated CMFs of different types of snowfalls. The graph a corresponds to event A13 (aggregate type) and the graph b to event G4 (grauple type), Both cases are listed in Table 1.

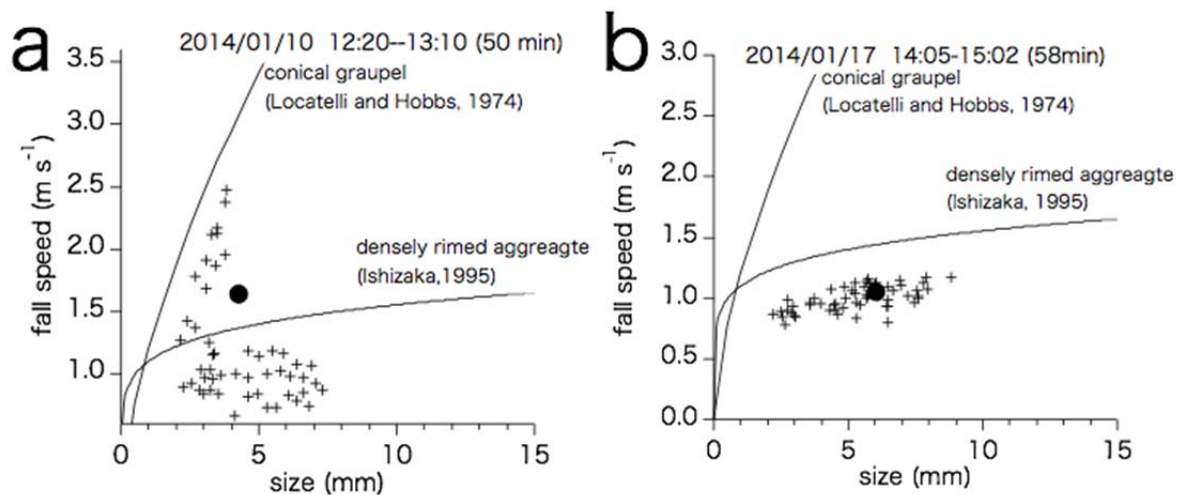


Figure 3: The distributions of 1 min-CMFs and the integrated CMFs for the events. a: eliminated case, b: selected case.

5

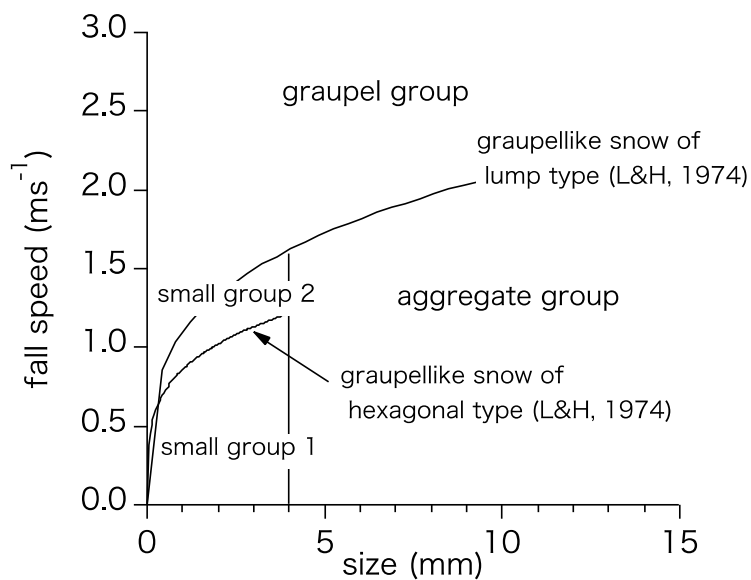


Figure 4: The boundaries for the group classification in the size-fall speed coordinates.

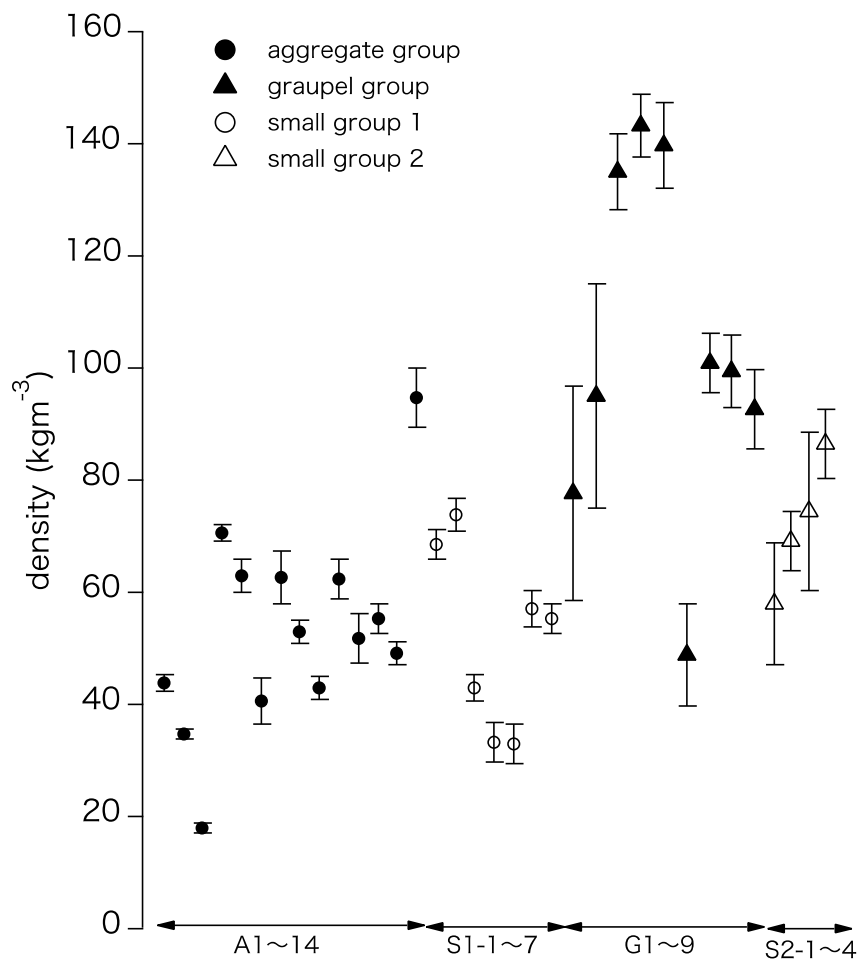


Figure 5: The measured snowfall densities arranged by the classified groups.

5

10

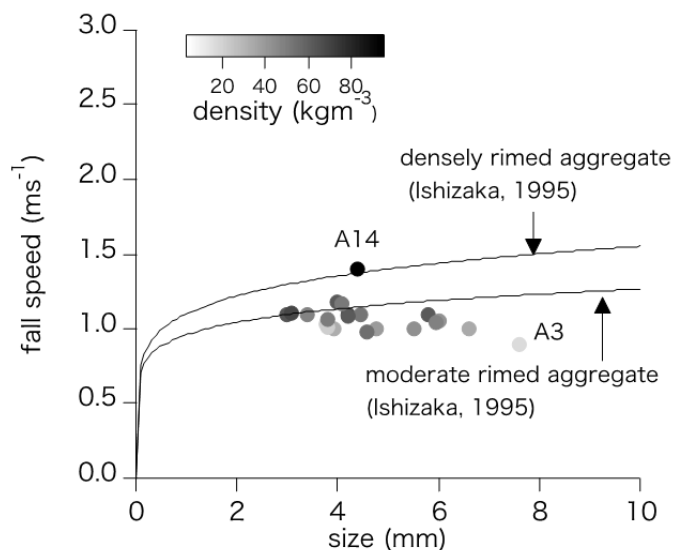
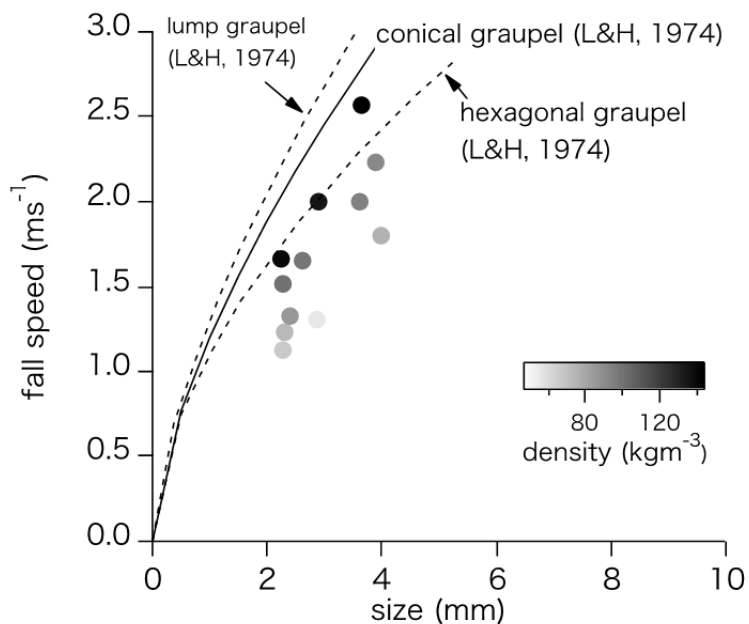


Figure 6: The CMFs of the snowfall events belonging to the aggregate group and small group 1. The density is expressed by grey-scale shading.



5 Figure 7: The CMFs of the snowfall events belonging to the graupel group and small group 2. The density is expressed by grey-scale shading.

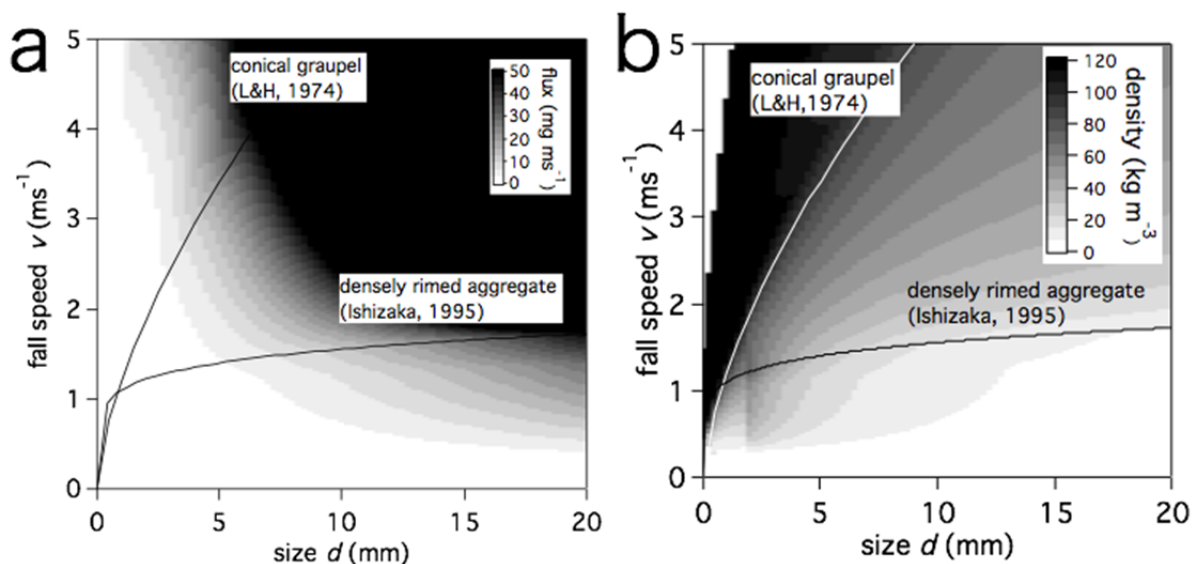


Figure 8: a: The mass flux chart. b: The density chart.

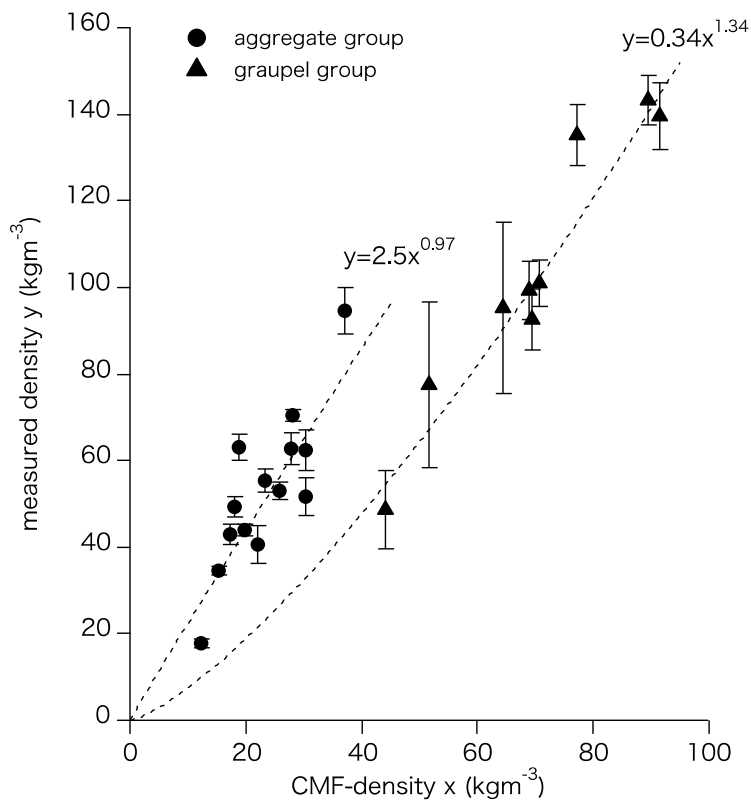


Figure 9: The relationships between the measured densities and the CMF densities for the aggregate group and for the graupel group.

5

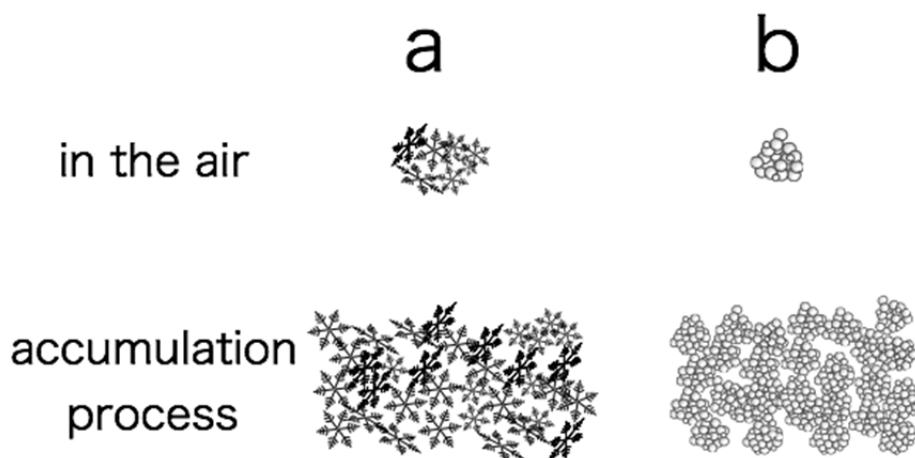
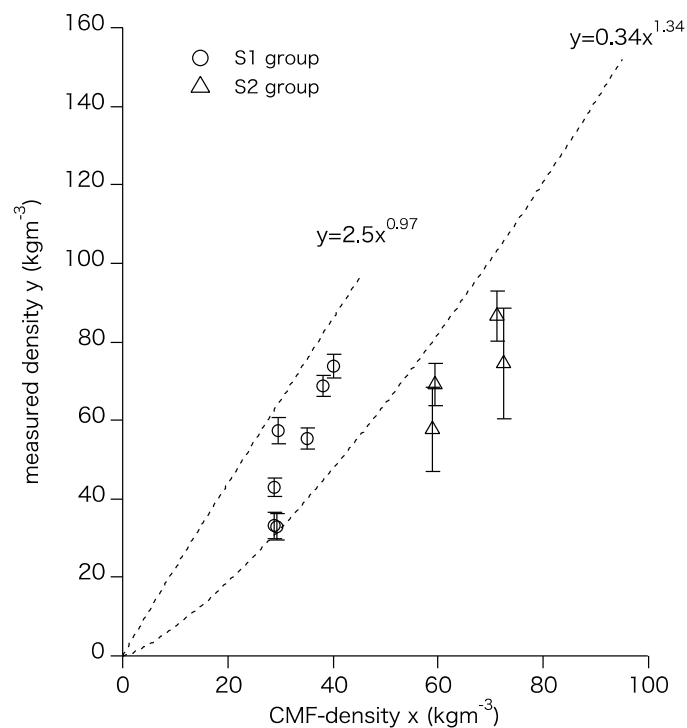


Figure 10: Schematic expression of the difference between the aggregate case (a) and the graupel case (b) in the packing process.



5 Figure 11: The relationships between measured densities and the CMF-densities for small group 1 and for small group 2. The curves are the fitted curves for the aggregate group and for the graupel group.